

# Yttrium Complexes Supported by Linked Bis(amide) Ligand: Synthesis, Structure, and Catalytic Activity in the Ring-Opening Polymerization of Cyclic Esters

Tatyana V. Mahrova,<sup>†</sup> Georgy K. Fukin,<sup>†</sup> Anton V. Cherkasov,<sup>†</sup> Alexander A. Trifonov,<sup>\*†</sup> Nouredine Ajellal,<sup>‡</sup> and Jean-François Carpentier<sup>\*\*‡</sup>

G.A. Razuvaev Institute of Organometallic Chemistry of Russian Academy of Sciences, Tropinina 49, GSP-445, 603950 Nizhny Novgorod, Russia, and Organometallics and Catalysis, Institute of Chemistry, UMR 6226 CNRS, University of Rennes 1, 35042 Rennes Cedex, France

Received December 22, 2008

A series of new yttrium complexes supported by the bulky enedi-amido dianionic ligand DAB<sup>2-</sup> (DAB<sup>2-</sup> = (2,6-C<sub>6</sub>H<sub>3</sub>iPr<sub>2</sub>)NC(Me)=C(Me)N(2,6-C<sub>6</sub>H<sub>3</sub>iPr<sub>2</sub>)<sup>2-</sup>), that is, {DAB}Y(THF)<sub>2</sub>(μ-Cl)<sub>2</sub>Li(THF)<sub>2</sub> (**1**), {DAB}Y(OtBu)(THF)(DME) (**2**), and {{DAB}Y(BH<sub>4</sub>)<sub>2</sub>}{Li(DME)<sub>3</sub>} (**3**), was synthesized by salt metathesis. The complexes were isolated after recrystallization in 73, 66, and 52% yield, respectively, and characterized in solution by NMR and in the solid state by single-crystal X-ray diffraction studies. In complex **1**, the DAB<sup>2-</sup> ligand is bonded to the metal center via two covalent Y–N bonds, while in complexes **2** and **3** additional η<sup>2</sup>-coordination of the C=C bond to the metal atom is observed, both in solution and in the solid state. The *tert*-butoxide and borohydride complexes **2** and **3** act as monoinitiators for the room temperature ring-opening polymerization of racemic lactide and β-butyrolactone, providing atactic polymers with controlled molecular weights and relatively narrow polydispersities (*M<sub>w</sub>*/*M<sub>n</sub>* = 1.15–1.82). Effectively immortal ROP of lactide with as many as 50 equiv of isopropanol per metal center was performed using complex **2** as the catalyst.

## Introduction

Aliphatic polyesters are an attractive class of thermoplastics thanks to their usual biodegradable and biocompatible nature. Within the growing global sustainability concern, the possibility to prepare some of these materials from renewable resources has proven to be of increasing importance and opened commercial perspectives for a range of applications (e.g., single-use packaging materials, biomedical systems).<sup>1</sup> Ring-opening polymerization (ROP) of cyclic esters, promoted notably (but not only) by single-site metal-based initiators/catalysts that operate via coordination/insertion pathways, is definitely the most useful route for preparing polyesters with good control over polymer molecular weight,

polydispersity, and microstructure.<sup>2</sup> The development over the past two decades of various types of metal catalysts for the ROP of cyclic esters has demonstrated the crucial influence that both the ancillary ligand and the initiating group exert on the polymerization performance. Among the large variety of metal complexes investigated, group 3 metals and lanthanide derivatives,<sup>2,3</sup> in particular complexes supported by dianionic linked bis(phenolate) ligands,<sup>4</sup> have been shown to be especially efficient. On the other hand, the *N*-containing analogues remain much less explored.<sup>5</sup> Recently, we have reported on original lanthanide borohydride<sup>6</sup> and alkoxide<sup>7</sup> complexes supported by bulky guanidinate ligands that initiate the “controlled-living” ROP of racemic lactide and β-butyrolactone. Herein we describe the synthesis and structural features of new yttrium borohydride and alkoxide complexes supported by a rigid dianionic bis(amide)

\* To whom correspondence should be addressed. Fax: (+33)223236939 (J.-F.C.), (+7)8314621497 (A.A.T.). E-mail: jcarpent@univ-rennes1.fr (J.-F.C.), trif@iomc.ras.ru (A.A.T.).

<sup>†</sup> Russian Academy of Sciences.

<sup>\*\*</sup> University of Rennes 1.

(1) (a) Mecking, S. *Angew. Chem., Int. Ed.* **2004**, *43*, 1078–1085. (b) Drumright, R. E.; Gruber, P. R.; Henton, D. E. *Adv. Mater.* **2000**, *12*, 1841–1846. (c) Auras, R.; Harte, B.; Selke, S. *Macromol. Biosci.* **2004**, *4*, 835–864. (d) Ha, C.-S.; Gardella, J. A. *Chem. Rev.* **2005**, *105*, 4205–4232.

(2) (a) O’Keefe, B. J.; Hillmyer, M. A.; Tolman, W. B. *J. Chem. Soc., Dalton Trans.* **2001**, 2215–2224. (b) Dechy-Cabaret, O.; Martin-Vaca, B.; Bourissou, D. *Chem. Rev.* **2004**, *104*, 6147–6176. (c) Dove, A. P. *Chem. Commun.* **2008**, 6446–6470.

(3) Amgoune, A.; Thomas, C. M.; Carpentier, J.-F. *Pure Appl. Chem.* **2007**, *79*, 2013–2030.

ligand derived from the 1,4-diaza-1,3-butadiene (DAB) framework. Their catalytic performances in the ROP of racemic lactide and  $\beta$ -butyrolactone have been explored as well.

## Experimental Section

**General Conditions.** All manipulations requiring a dry atmosphere were performed under a purified argon atmosphere using standard Schlenk techniques or in a glovebox. Anhydrous  $\text{YCl}_3$ ,<sup>8</sup>  $\text{Y}(\text{BH}_4)_3(\text{THF})_2$ ,<sup>9</sup> and  $\text{DAB}$ <sup>10</sup> were prepared according to literature procedures. *tert*-BuOK and  $\text{NaBH}_4$  were purchased from Acros and used as received. Solvents (toluene, THF, hexane) were freshly distilled from Na/K alloy under nitrogen and degassed thoroughly by freeze–vacuum–thaw cycles prior to use.  $\text{CH}_2\text{Cl}_2$  was dried over  $\text{CaH}_2$ , distilled twice, and degassed by freeze–vacuum–thaw cycles prior to use. Deuterated solvents, except  $\text{CDCl}_3$ , were freshly distilled from Na/K amalgam under argon and degassed prior to use. Racemic lactide (Aldrich) was recrystallized twice from dry toluene and then sublimed under vacuum at 50 °C. Racemic  $\beta$ -butyrolactone (Aldrich) was freshly distilled from  $\text{CaH}_2$  under nitrogen and degassed thoroughly by freeze–vacuum–thaw cycles prior to use.

**Instruments and Measurements.** IR spectra were recorded as Nujol mulls on a Bruker-Vertex 70 spectrophotometer. NMR spectra were recorded on Bruker AM-500, Bruker Avance DRX-400 and DPX-200 spectrometers in  $[\text{D}_6]$ benzene,  $[\text{D}_8]$ toluene, or  $\text{CDCl}_3$  at 20 °C, unless otherwise stated. C,H elemental analysis was performed by the microanalytical laboratory of IOMC. Lanthanide metal analysis was carried out by complexometric titration. Size exclusion chromatography (SEC) of PLAs and PHBs was performed in THF at 20 °C using a Polymer Laboratories PL50 apparatus equipped with PLgel 5  $\mu\text{m}$  MIXED-C 300  $\times$  7.5 mm columns and combined RI and Dual angle LS (PL-LS 45/90°) detectors. The number average molecular masses ( $M_n$ ) and polydispersity index ( $M_w/M_n$ ) of the polymers were calculated with reference to a

universal calibration versus polystyrene standards.  $M_n$  values of PLAs were corrected with a Mark–Houwink factor of 0.58 to account for the difference in hydrodynamic volumes between polystyrene and polylactide.<sup>11</sup> The microstructure of PLAs was determined by homodecoupling  $^1\text{H}$  NMR spectroscopy at 20 °C in  $\text{CDCl}_3$  with a Bruker AC-500 spectrometer. The microstructure of PHBs was determined by analyzing the carbonyl region of  $^{13}\text{C}\{^1\text{H}\}$  NMR spectra at 20 °C in  $\text{CDCl}_3$  with a Bruker AC-500 spectrometer operating at 125 MHz.<sup>12</sup>

**Synthesis of  $\{\text{DAB}\}\text{Y}(\text{THF})_2(\mu\text{-Cl})_2\text{Li}(\text{THF})_2$  (1).** A solution of DAB (1.00 g, 2.47 mmol) in THF (50 mL) was added to Li shavings (0.035 g, 5.00 mmol), and the reaction mixture was stirred at room temperature for 3 days until complete dissolution of the metal. The resulting red-orange solution was filtered and added slowly to a suspension of  $\text{YCl}_3$  (0.480 g, 2.46 mmol) in THF (15 mL). The reaction mixture was stirred at room temperature for 45 min. The solvent was evaporated under vacuum, the resulting solid residue was extracted with toluene (2  $\times$  20 mL), and the extracts were filtered. Volatiles were removed under vacuum, and the resulting solid was recrystallized from a THF–hexane (1:5) mixture. The mother liquor was separated by decantation, and the yellow-orange crystals were washed with cold hexane and dried in vacuum to afford analytically pure **1** (1.54 g, 73%).  $^1\text{H}$  NMR (200 MHz,  $[\text{D}_6]$ benzene, 293 K):  $\delta$  = 1.33 (br s, 24 H,  $\text{CHCH}_3$ ), 1.46 (br s, 16H,  $\beta\text{-CH}_2$ , THF), 1.90 (br s, 6H,  $\text{CH}_3\text{C}=\text{C}$ ), 3.62 (br s, 16H,  $\alpha\text{-CH}_2$ , THF), 3.98 (br s, 4 H,  $\text{CH}(\text{CH}_3)_2$ ), 6.99–7.27 (m, 6H, Arom.).  $^1\text{H}$  NMR (400 MHz,  $[\text{D}_8]$ toluene, 241 K):  $\delta$  = 1.28, 1.34, 1.42, 1.77 (d,  $^3J_{\text{H-H}} = 6.5$  Hz, together 24H,  $\text{CH}(\text{CH}_3)_2$ ), 1.55 (br s, 16H,  $\beta\text{-CH}_2$ , THF), 1.66 (s, 6H,  $\text{CH}_3\text{C}=\text{C}$ ), 3.38, 3.50 (br s, together 16H,  $\alpha\text{-CH}_2$ , THF), 3.80, 4.01 (br s, 2H,  $\text{CH}(\text{CH}_3)_2$ ), 6.99–7.35 (m, 6H, Arom.).  $^{13}\text{C}\{^1\text{H}\}$  NMR (100 MHz,  $[\text{D}_6]$ benzene):  $\delta$  = 18.0 (s,  $=\text{CCH}_3$ ), 23.9, 24.2, 25.6, 25.9 (s,  $\text{CHCH}_3$ ), 25.1 (s,  $\beta\text{-C}$ , THF), 27.9, 28.1 (s,  $\text{CHCH}_3$ ), 68.4 (s,  $\alpha\text{-C}$ , THF), 118.0 (s,  $=\text{CCH}_3$ ), 121.7, 122.1, 123.4, 145.1, 146.9, 150.6 (s, Ar).  $^7\text{Li}$  NMR (155.5 MHz,  $[\text{D}_6]$ benzene, 293 K):  $\delta$  = 2.2. IR (Nujol, KBr):  $\tilde{\nu}$  = 3050 (m), 1640 (s), 1590 (s), 1437 (s), 1363 (s), 1327 (m), 1256(m), 1184(m), 1120 (s), 934 (m), 762 (s)  $\text{cm}^{-1}$ . Anal. Calcd (%) for  $\text{C}_{44}\text{H}_{72}\text{Cl}_2\text{LiN}_2\text{O}_4\text{Y}$  (859.8): C, 61.46; H, 8.37; Y, 10.33. Found: C, 61.09; H, 8.66; Y, 10.67.

**Synthesis of  $\{\text{DAB}\}\text{Y}(\text{OtBu})(\text{THF})(\text{DME})$  (2).** A solution of *t*BuOK (0.083 g, 0.74 mmol) in THF (10 mL) was added to a solution of **1** (0.64 g, 0.74 mmol) in THF (25 mL) at room temperature, and the reaction mixture was stirred overnight. THF was evaporated under vacuum, and the solid residue was extracted with toluene (2  $\times$  20 mL). The extracts were filtered, toluene was removed under vacuum, and the resulting solid was recrystallized from a DME–hexane (1:4) mixture. The orange crystals were washed with cold hexane and dried in vacuum to afford analytically pure **2** (0.36 g, 66%).  $^1\text{H}$  NMR (200 MHz,  $[\text{D}_6]$ benzene, 293 K):  $\delta$  = 1.27 (d,  $^3J_{\text{H-H}} = 6.8$  Hz, 12H,  $\text{CH}(\text{CH}_3)_2$ ), 1.32 (s, 9H,  $(\text{CH}_3)_3\text{C}$ ), 1.39 (br s, 4H,  $\beta\text{-CH}_2$ , THF), 1.51 (d,  $^3J_{\text{H-H}} = 6.8$  Hz, 12H,  $\text{CH}(\text{CH}_3)_2$ ), 1.95 (s, 6H,  $\text{CH}_3\text{C}=\text{C}$ ), 2.55 (s, 4H,  $\text{CH}_2\text{O}$ , DME), 3.15 (s, 6H,  $\text{CH}_3\text{O}$ , DME), 3.57 (br s, 4H,  $\alpha\text{-CH}_2$ , THF), 3.89 (br sept,  $^3J_{\text{H-H}} = 6.8$  Hz, 4H,  $\text{CH}(\text{CH}_3)_2$ ), 7.11–7.33 (m, 6H, Arom.).  $^{13}\text{C}\{^1\text{H}\}$  NMR (50 MHz,  $[\text{D}_6]$ benzene, 293 K):  $\delta$  = 18.6 (s,  $=\text{CCH}_3$ ), 23.7, 23.9, 24.1, 25.4 (s,  $\text{CHCH}_3$ ), 25.6 (s,  $\beta\text{-C}$ , THF), 27.9 (s,  $\text{CHCH}_3$ ), 33.9 (s,  $\text{CHCH}_3$ ), 34.7 (s,  $\text{OCCH}_3$ ), 61.5 (s,  $\text{OCH}_3$ , DME), 67.8 (s,  $\alpha\text{-C}$ , THF), 69.8 ( $\text{OCH}_2$ , DME), 70.1 ( $\text{OCCH}_3$ ),

- (4) (a) Cai, C.-X.; Amgoune, A.; Lehmann, C. W.; Carpentier, J.-F. *Chem. Commun.* **2004**, 330–331. (b) Amgoune, A.; Thomas, C. M.; Roisnel, T.; Carpentier, J.-F. *Chem.–Eur. J.* **2006**, *12*, 169–179. (c) Castro, P. M.; Zhao, G.; Amgoune, A.; Thomas, C. M.; Carpentier, J.-F. *Chem. Commun.* **2006**, 4509–4511. (d) Amgoune, A.; Thomas, C. M.; Ilinca, S.; Roisnel, T.; Carpentier, J.-F. *Angew. Chem., Int. Ed.* **2006**, *45*, 2782–2784. (e) Amgoune, A.; Thomas, C. M.; Carpentier, J.-F. *Macromol. Rapid Commun.* **2007**, *28*, 693–697. (f) Ma, H.; Spaniol, T. P.; Okuda, J. *Dalton Trans.* **2003**, 4770–4780. (g) Ma, H.; Okuda, J. *Macromolecules* **2005**, *38*, 2665–2673. (h) Ma, H.; Spaniol, T. P.; Okuda, J. *Angew. Chem., Int. Ed.* **2006**, *45*, 7818–7821. (i) Bonnet, F.; Cowley, A. R.; Mountford, P. *Inorg. Chem.* **2005**, *44*, 9046–9055. (j) Dyer, H. E.; Huijster, S.; Schwarz, A. D.; Wang, C.; Duchateau, R.; Mountford, P. *Dalton Trans.* **2008**, 32–35. (k) Liu, X.; Chang, X.; Tang, T.; Hu, N.; Pei, F.; Cui, D.; Chen, X.; Jing, X. *Organometallics* **2007**, *26*, 2747–2757.
- (5) (a) Platel, R. P.; Hodgson, L. M.; White, A. J. P.; Williams, C. K. *Organometallics* **2007**, *26*, 4955–4969. (b) Carver, C. T.; Monreal, M. J.; Diaconescu, P. L. *Organometallics* **2008**, *27*, 363–370. (c) Cloke, F. G. N.; Elvidge, B. R.; Hitchcock, P. B.; Lamarche, V. M. E. *J. Chem. Soc., Dalton Trans.* **2002**, 2413–2414. (d) Avent, A. G.; Cloke, F. G. N.; Elvidge, B. R.; Hitchcock, P. B. *Dalton Trans.* **2004**, 1083–1096.
- (6) Skvortsov, G. G.; Yakovenko, M. V.; Castro, P. M.; Fukin, G. K.; Cherkasov, A. V.; Carpentier, J.-F.; Trifonov, A. A. *Eur. J. Inorg. Chem.* **2007**, 3260–3267.
- (7) Ajellal, N.; Lyubov, D. M.; Sinenkov, M. A.; Fukin, G. K.; Cherkasov, A. V.; Thomas, C. M.; Carpentier, J.-F.; Trifonov, A. A. *Chem.–Eur. J.* **2008**, *14*, 5440–5448.
- (8) Manzer, L. E. *Inorg. Chem.* **1978**, *17*, 1552–1558.
- (9) Mirsaidov, U.; Shaimuradov, I.; Hikmatov, M. *Zh. Neorg. Khim. (Russ. J. Inorg. Chem.)* **1986**, *31*, 1321–1326.
- (10) Svoboda, M.; Dieck, H. T. *J. Organomet. Chem.* **1980**, *191*, 321–327.

- (11) Barakat, I.; Dubois, P.; Jerome, R.; Teyssié, P. *J. Polym. Sci., A: Polym. Chem.* **1993**, *31*, 505–514.
- (12) (a) Giesbrecht, G. R.; Whitener, G. D.; Arnold, J. *J. Chem. Soc., Dalton Trans.* **2001**, 923–927. (b) Ajellal, N.; Bouyahy, M.; Amgoune, A.; Thomas, C. M.; Bondon, A.; Pillin, I.; Grohens, Y.; Carpentier, J.-F. *Macromolecules* **2009**, *42*, 987–993.

**Table 1.** Crystallographic Data and Structure Refinement Details for Complexes **1–3**

	1	2	3
empirical formula	C <sub>44</sub> H <sub>72</sub> Cl <sub>2</sub> LiN <sub>2</sub> O <sub>4</sub> Y	C <sub>40</sub> H <sub>67</sub> N <sub>2</sub> O <sub>4</sub> Y	C <sub>40</sub> H <sub>78</sub> B <sub>2</sub> LiN <sub>2</sub> O <sub>6</sub> Y
formula weight	859.79	728.87	800.51
crystal size, mm	0.61 × 0.54 × 0.39	0.51 × 0.36 × 0.28	0.48 × 0.32 × 0.14
<i>T</i> (K)	100(2)	100(2)	100(2)
space group	<i>P</i> 2(1)/ <i>c</i>	<i>P</i> 2(1)/ <i>c</i>	<i>Pbca</i>
<i>A</i> (Å)	10.7612(4)	14.1204(4)	16.0810(4)
<i>B</i> (Å)	21.5649(7)	16.7843(5)	16.8673(4)
<i>C</i> (Å)	20.1727(7)	17.0290(5)	35.3301(8)
$\alpha$ (deg)	90	90	90
$\beta$ (deg)	103.847(1)	95.031(1)	90
$\gamma$ (deg)	90	90	90
<i>V</i> (Å <sup>3</sup> )	4545.3(3)	4020.3(2)	9583.0(4)
<i>Z</i>	4	4	8
calculated density (mg/m <sup>3</sup> )	1.256	1.204	1.110
absorption coefficient (mm <sup>-1</sup> )	1.441	1.490	1.257
<i>T</i> <sub>min</sub> / <i>T</i> <sub>max</sub>	0.4734/0.6033	0.5171/0.6805	0.5837/0.8437
<i>F</i> (000)	1832	1568	3456
2 $\theta$ (deg)	55	52	55
unique reflections collected ( <i>R</i> <sub>int</sub> )	10419 (0.0259)	7885 (0.0318)	10988 (0.0980)
<i>R</i> <sub>1</sub> ( <i>I</i> > 2 $\sigma$ ( <i>I</i> ))	0.0294	0.0443	0.0474
w <i>R</i> <sub>2</sub> (all data)	0.0700	0.1119	0.1219
parameters	511	403	501
goodness-of-fit on <i>F</i> <sup>2</sup>	0.971	1.070	1.013
largest diff. hole and peak (e/Å <sup>3</sup> )	−0.352/0.781	−1.157/1.157	−0.488/0.549

113.8 (d, <sup>1</sup>*J*<sub>Y–C</sub> = 2.4 Hz, =C–N), 120.7, 127.5, 128.0, 138.8, 144.3 (s, Arom.), 149.7 (d, <sup>2</sup>*J*<sub>Y–C</sub> = 2.3 Hz, C ipso). IR (Nujol, KBr):  $\tilde{\nu}$  = 3060 (m), 1642 (m), 1588 (w), 1364 (s), 1250 (m), 1210 (m), 1121 (s), 1085 (m), 935 (w), 870 (w), 762 (s), 736 (m) cm<sup>-1</sup>. Anal. Calcd (%) for C<sub>40</sub>H<sub>67</sub>N<sub>2</sub>O<sub>4</sub>Y (728.8): C 65.92, H 9.19, Y 12.19; found: C 65.61; H 8.80; Y 11.90.

**Synthesis of {{DAB}Y(BH<sub>4</sub>)<sub>2</sub>}{Li(DME)<sub>3</sub>} (3).** A solution of [DAB]Li<sub>2</sub>, obtained by the reaction of DAB (1.00 g, 2.47 mmol) and Li metal (0.035 g, 5.00 mmol) in THF (50 mL), was slowly added to a suspension of Y(BH<sub>4</sub>)<sub>3</sub>(THF)<sub>2</sub> (0.68 g, 2.47 mmol) in THF (15 mL). The reaction mixture was stirred at room temperature overnight. THF was removed under vacuum and the solid residue was extracted with toluene (2 × 20 mL). Filtration of the extracts, evaporation of toluene under vacuum and recrystallization of the resulting solid from a DME-hexane (1:5) mixture afforded **3** as yellow crystals (1.02 g, 52%). <sup>1</sup>H NMR (200 MHz, [D<sub>6</sub>]benzene, 293 K):  $\delta$  = 0.05 (br s, 1H, BH<sub>4</sub>), 0.42 (br s, 3H, BH<sub>4</sub>), 1.29 (d, <sup>3</sup>*J*<sub>H–H</sub> = 6.8 Hz, 12H, CH(CH<sub>3</sub>)<sub>2</sub>), 1.43 (d, <sup>3</sup>*J*<sub>H–H</sub> = 6.8 Hz, 12H, CH(CH<sub>3</sub>)<sub>2</sub>), 1.89 (s, 6H, CH<sub>3</sub>C=), 2.88 (s, 12H, CH<sub>2</sub>O, DME), 2.97 (s, 18H, CH<sub>3</sub>O, DME), 3.91 (sept, <sup>3</sup>*J*<sub>H–H</sub> = 6.8 Hz, 4H, CH(CH<sub>3</sub>)<sub>2</sub>), 7.03–7.20 (m, 6H, Arom.). <sup>13</sup>C{<sup>1</sup>H} NMR (50 MHz, [D<sub>6</sub>]benzene, 293 K): 18.1 (s, =CCH<sub>3</sub>), 24.1 (s, CHCH<sub>3</sub>), 25.4 (s, CHCH<sub>3</sub>), 28.0 (s, CHCH<sub>3</sub>), 59.3 (s, OCH<sub>3</sub>, DME), 70.5 (s, OCH<sub>2</sub>, DME), 113.9 (d, <sup>1</sup>*J*<sub>Y–C</sub> = 2.4 Hz, =C–N), 121.5, 123.1, 128.9, 143.2, 144.2 (s, Arom.), 148.7 (d, <sup>2</sup>*J*<sub>Y–C</sub> = 4.8 Hz, C ipso). <sup>7</sup>Li NMR (77.7 MHz, [D<sub>6</sub>]benzene):  $\delta$  = 0.8. <sup>11</sup>B NMR (64.2 MHz, [D<sub>6</sub>]benzene):  $\delta$  = 66.7. IR (Nujol, KBr):  $\tilde{\nu}$  = 3050 (m), 2427 (s), 2215 (s), 2160 (s), 1587 (w), 1312 (m), 1257 (s), 1189 (m), 1119 (m), 1081 (m), 1024 (m), 946 (m), 931 (m), 892 (m), 866 (m) cm<sup>-1</sup>. Anal. Calcd (%) for C<sub>40</sub>H<sub>78</sub>B<sub>2</sub>LiN<sub>2</sub>O<sub>6</sub>Y (800.5): C, 60.01; H, 9.74; Y, 11.10. Found: C, 59.61; H, 9.89; Y, 11.30.

**Crystal Structure Determination of 1, 2, and 3.** Crystals of **1**, **2**, and **3** suitable for X-ray diffraction analysis were obtained by recrystallization of purified products (see text and Experimental Section). The data were collected on a SMART APEX diffractometer (graphite-monochromated, Mo K $\alpha$ -radiation,  $\omega$ - and  $\theta$ -scan

technique,  $\lambda$  = 0.71073 Å). The structures were solved by direct methods and were refined on *F*<sup>2</sup> using SHELXTL<sup>13</sup> package. All non-hydrogen atoms were refined anisotropically. The hydrogen atoms in **1–3** were placed in calculated positions and were refined in the riding model except hydrogens in BH<sub>4</sub> groups in **3** which were found from Fourier syntheses of electron density and were refined isotropically. SADABS<sup>14</sup> was used to perform area-detector scaling and absorption corrections.

Crystal data and details of data collection and structure refinement for the different compounds are given in Table 1. Main crystallographic data (excluding structure factors) are available as Supporting Information, as CIF files. CCDC-713634 (**1**), CCDC-713635 (**2**), and CCDC-713636 (**3**) contain the supplementary crystallographic data for this paper. These data can be obtained free of charge via [www.ccdc.cam.ac.uk/conts/retrieving.html](http://www.ccdc.cam.ac.uk/conts/retrieving.html) (or from the Cambridge Crystallographic Data Centre, 12 Union Road, Cambridge CB21EZ, UK; fax, (+44) 1223-336-033; or deposit@ccdc.cam.ac.uk).

**Typical Procedure for the Polymerization of *rac*-Lactide.** In a typical experiment (Table 2, entry 3), in a glovebox, a Schlenk flask was charged with a solution of initiator **2** (6.3 mg, 8.7  $\mu$ mol) in THF (0.20 mL). To this solution, *rac*-lactide (125 mg, 0.87 mmol, 100 equiv) in THF (0.67 mL) was added rapidly (isopropanol was added at this stage for experiments conducted under “immortal” conditions). The mixture was immediately stirred with a magnetic stir bar at 20 °C for 14 h. After an aliquot of the crude material was sampled by pipet for determining monomer conversion by <sup>1</sup>H NMR, the reaction was quenched with acidic methanol (ca. 1 mL of a 1.2 M HCl solution in MeOH), and the polymer was precipitated with excess methanol (ca. 50 mL). The polymer was then filtered and dried under vacuum to constant weight.

**Typical Procedure for Polymerization of *rac*- $\beta$ -Butyrolactone.** In a typical experiment (Table 3, entry 5), in a glovebox, a Schlenk flask was charged with a solution of initiator **2** (6.3 mg, 8.7  $\mu$ mol) in toluene (0.19 mL). To this solution, *rac*- $\beta$ -butyrolactone (74.8 mg, 0.87 mmol, 100 equiv) in toluene (0.10 mL) was added rapidly. The mixture was immediately stirred with a magnetic stir bar at 20 °C. The reaction was processed and worked-up similarly as described above for lactide polymerization.

(13) Sheldrick, G. M. *SHELXTL, Structure Determination Software Suite*, version 6.12; Bruker AXS: Madison, WI, 2000.

(14) Sheldrick, G. M. *SADABS, Bruker/Siemens Area Detector Absorption Correction Program*; version 2.01; Bruker AXS: Madison, WI, 1998.

**Table 2.** Ring-Opening Polymerization of *rac*-Lactide Promoted by Complexes **2** and **3**<sup>a</sup>

entry	complex	[LA]/[Y]	[iPrOH]/[Y]	solvent	time <sup>b</sup> (h)	conv. (%)	$M_{n,calc}^c$ ( $\times 10^3$ )	$M_{n,exp}^d$ ( $\times 10^3$ )	$M_w/M_n^d$
1	<b>3</b>	150	0	toluene	4	92	13.2	13.4	1.24
2	<b>3</b>	100	0	THF	4	64	9.2	7.0	1.18
3	<b>2</b>	100	0	toluene	16	>99	14.3	10.7	1.80
4	<b>2</b>	500	0	toluene	16	>99	72.0	42.4	1.44
5	<b>2</b>	100	0	THF	16	>99	14.3	9.2	1.55
6	<b>2</b>	500	0	THF	16	81	58.3	24.8	1.82
7	<b>2</b>	500	5	THF	16	>99	14.3	10.0	1.72
8	<b>2</b>	500	10	THF	16	>99	7.2	7.0	1.52
9	<b>2</b>	500	50	THF	16	>99	1.4	3.3	1.41
10	<b>2</b>	1000	5	THF	24	90	25.9	21.2	1.54
11	<b>2</b>	2000	5	THF	30	78	45.0	41.2	1.65

<sup>a</sup> All reactions performed at 20 °C with  $[rac-LA] = 1.0$  M. <sup>b</sup> Reaction time was not necessarily optimized. <sup>c</sup>  $M_n$  ( $g \cdot mol^{-1}$ ) of PLAs calculated from  $M_{n,calc} = 144 \times ([LA]/[Y]) \times conv.$  <sup>d</sup>  $M_n$  ( $g \cdot mol^{-1}$ ) (corrected, see the Experimental Section) and  $M_w/M_n$  of PLAs determined by SEC-RI using polystyrene standards.

**Table 3.** Ring-Opening Polymerization of *rac*-BBL Promoted by Complexes **2** and **3**<sup>a</sup>

entry	complex	[BBL]/[Y]	solvent	time (h)	conv. (%)	$M_{n,calc}^b$ ( $\times 10^3$ )	$M_{n,exp}^c$ ( $\times 10^3$ )	$M_w/M_n^c$
1	<b>3</b>	100	toluene	14	61	5.2	3.9	1.25
2	<b>3</b>	200	toluene	20	41	7.0	4.6	1.15
3	<b>3</b>	500	toluene	48	14	6.0	4.5	1.30
4	<b>2</b>	100	THF	18	42	3.6	4.0	1.17
5	<b>2</b>	100	toluene	18	67	5.8	4.2	1.18

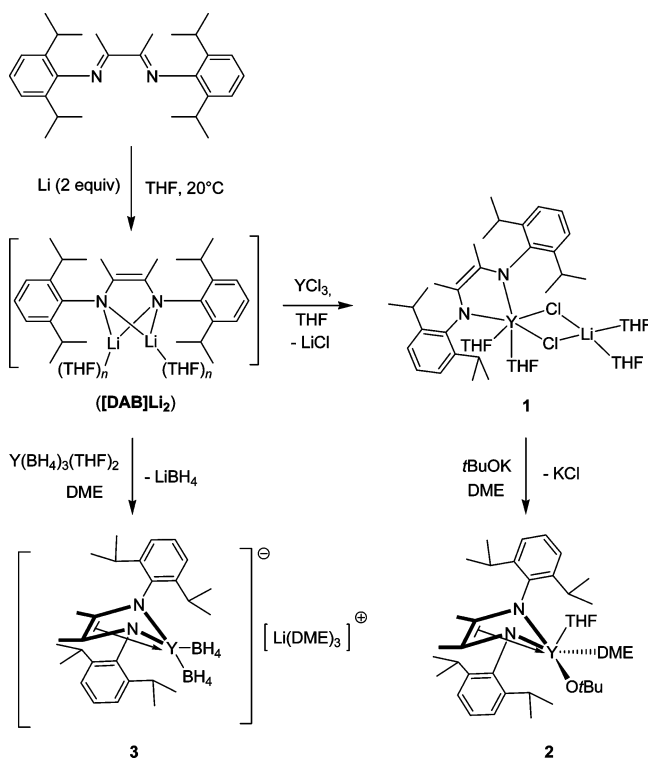
<sup>a</sup> All reactions performed with  $[rac-BBL] = 3.0$  M at 20 °C. <sup>b</sup>  $M_n$  ( $g \cdot mol^{-1}$ ) of PHBs calculated from  $M_{n,calc} = 86 \times ([BBL]/[Y]) \times conversion$  (BBL). <sup>c</sup>  $M_n$  ( $g \cdot mol^{-1}$ ) and  $M_w/M_n$  of PHBs determined by SEC-RI using polystyrene standards.

## Results and Discussion

**Synthesis and Solution NMR Studies of Yttrium–DAB Complexes 1–3.** The easily accessible chelating dianionic bis(amide) ligand ( $DAB^{2-} = (2,6-C_6H_3iPr_2)NC(Me)=C(Me)-N(2,6-C_6H_3iPr_2)^{2-}$ ), capable of coordinating onto lanthanide metals and to form eventually rigid metallocycles, was prepared from the 1,4-diaza-1,3-butadiene framework bearing bulky 2,6-di-isopropylphenyl substituents at the nitrogen atoms. The reaction of the dilithium derivative  $[DAB]Li_2$ , which was obtained in situ by reduction of the neutral diimine precursor with a 2-fold molar excess of lithium metal in THF, with an equimolar amount of  $YCl_3$ , afforded the chloro complex  $\{DAB\}Y(THF)_2(\mu-Cl)_2Li(THF)_2$  (**1**) in 73% yield (Scheme 1). The reaction of complex **1** with 1 equiv of *t*BuOK was carried out in THF at room temperature. Separation of the precipitated KCl, evaporation of volatiles under vacuum, extraction of the resulting solid residue with toluene, and subsequent recrystallization from a DME–hexane mixture (1:4) allowed isolating complex  $\{DAB\}Y(OtBu)(THF)(DME)$  (**2**) in 66% yield (Scheme 1). For preparation of the related borohydride, in situ generated  $[DAB]Li_2$  was reacted with 1 equiv of  $Y(BH_4)_3(THF)_2$  in THF. Evaporation of volatiles under vacuum and extraction of the solid residue with toluene followed by recrystallization from a DME–hexane mixture (1:5) afforded complex  $\{DAB\}Y(BH_4)_2\{Li(DME)_3\}$  (**3**) in 52% yield (Scheme 1).

Complexes **1–3** were isolated as yellow-orange air- and moisture-sensitive crystals. All of those compounds were authenticated by elemental analyses, solution NMR studies, and single-crystal X-ray diffraction studies. Complexes **1–3** are well soluble in THF, DME, and toluene but insoluble in hexanes. The resonances in the  $^1H$  and  $^{13}C\{^1H\}$  spectra of complex **1** in  $[D_6]benzene$  at room temperature are noticeably broadened, reflecting the existence of a dynamic behavior in these conditions. Decrease of the temperature down to

### Scheme 1



241 K (in  $[D_8]toluene$ ) allowed freezing of this dynamic process, resulting in a set of sharp resonances, consistent with the expected structure (see the Experimental Section). The decoalescence of the broad singlet for the  $\alpha-CH_2$  THF hydrogens at 253 K in two sharp resonances indicates a labile THF ligand. Concomitant decoalescence (at 241 K) of the broad singlet for the methyl hydrogens of the *iso*-propyl groups in four doublets suggests slow rotation of 2,6- $C_6H_3iPr_2$  fragments. Unlike complex **1**, the room temperature  $^1H$  and  $^{13}C\{^1H\}$  NMR spectra of **2** and **3** present sharp resonances. It is noteworthy that, in complexes **2** and **3**, the C=C bond

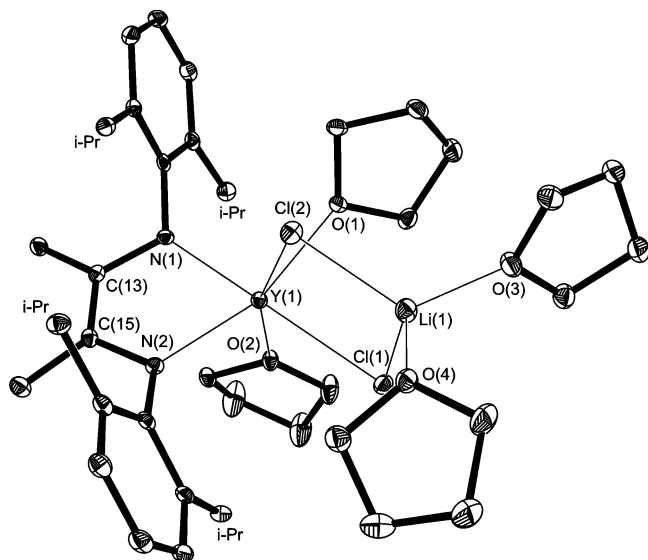


**Figure 1.** Molecular structure of  $\{\text{DAB}\}\text{Y}(\text{THF})_2(\mu\text{-Cl})_2\text{Li}(\text{THF})_2$  (**1**) with 30% ellipsoid probability; the methyl groups of the *t*Pr fragments are omitted for clarity. Selected distances (Å) and angles (deg): Y(1)–O(1) 2.422(1), Y(1)–O(2) 2.387(1), Y(1)–N(1) 2.247(1), Y(1)–N(2) 2.243(1), Y(1)–Cl(1) 2.716(1), Y(1)–Cl(2) 2.655(1), N(1)–C(13) 1.425(2), N(2)–C(15) 1.425(2), C(13)–C(15) 1.359(2), Li(1)–O(3) 1.936(3), Li(1)–O(4) 1.906(3), N(2)–Y(1)–N(1) 74.35(5), Cl(2)–Y(1)–Cl(1) 82.95(1), O(2)–Y(1)–O(1) 90.12(4).

of the enediamido  $\text{DAB}^{2-}$  fragment is  $\eta^2$ -coordinated onto the yttrium atom (vide infra). This coordination is evidenced by the observation in the  $^{13}\text{C}\{^1\text{H}\}$  NMR spectra of **2** and **3** (in  $[\text{D}_6]$ benzene) of doublets ( $\delta$  113.8 ppm,  $^1J_{\text{Y-C}} = 2.4$  Hz, and  $\delta$  113.9 ppm,  $^1J_{\text{Y-C}} = 2.4$  Hz, respectively) for these carbon atoms, reflecting their coupling with the yttrium atom. For complex **1**, in which coordination of the  $\text{C}=\text{C}$  bond onto the yttrium atom was not observed in the solid state (vide infra), the corresponding carbons appear in the  $^{13}\text{C}\{^1\text{H}\}$  NMR spectrum as a singlet at  $\delta$  118.0 ppm.

The presence of lithium in complexes **1** and **3** was confirmed by their  $^7\text{Li}$  NMR spectra which contain single resonances at  $\delta$  2.2 and 0.8 ppm, respectively. The  $^{11}\text{B}$  NMR spectrum of complex **3** features a single resonance at  $\delta$  66.7 ppm, while the hydrogen atoms of the  $\text{BH}_4^-$  anions appear in the  $^1\text{H}$  NMR spectrum as a set of two broad singlets with the integral intensity ratio 1:3. In the IR spectrum of complex **3**, the borohydride groups appear as three intensive absorption bands at  $\nu$  2427, 2215, and 2160  $\text{cm}^{-1}$ . These spectroscopic data for the borohydride moiety compare well to those observed in related yttrium–borohydride complexes.<sup>15</sup>

**X-ray Diffraction Studies of Complexes 1–3.** Single crystals of complex **1** suitable for X-ray diffraction studies were obtained by slow condensation of hexane into a THF solution of **1** at room temperature. The molecular structure of **1** is depicted in Figure 1, and the crystal and structural refinement data are summarized in Table 1. Complex **1** crystallizes in the monoclinic space group  $P2_1/c$  with four molecules in the unit cell and is a monomeric *ate* complex with the yttrium and lithium atoms linked by two  $\mu$ -bridging

chloride ligands. The molecular structure shows the metal center in a distorted octahedral environment, hexacoordinated by two nitrogen atoms of the chelating  $\text{DAB}^{2-}$  ligand, two chloride anions, and two oxygen atoms of two THF molecules (Figure 1). The five-membered metallacycle is practically planar. The deviation of the yttrium atom from the mean metallacycle plane is 0.049 Å, and the dihedral angle between the N(1)Y(1)N(2) and the N(1)C(13)C(15)N(2) planes is 7.8°. The Y–N bond lengths in **1** (2.243(1) and 2.247(1) Å) compare well to the values reported for six-coordinated yttrium–amido complexes.<sup>16</sup> The geometry of the planar NCCN fragment (atoms deviation from the mean plane = 0.001 Å) in **1** is consistent with the dianionic character of the  $\text{DAB}^{2-}$  ligand. The N–C bonds in the  $\text{DAB}^{2-}$  dianion of **1** (1.425(2) and 1.425(2) Å) are substantially elongated while the C–C bond (1.359(2) Å) is shortened, compared to the N=C (1.279(3) and 1.280(3) Å) and C–C bond distances (1.498(3) Å) in the parent neutral DAB molecule;<sup>17</sup> the C–C bond length is actually close to the values for the usual C=C double bonds.<sup>18</sup> The bonding situation within the  $\text{DAB}^{2-}$  fragment in **1** is similar to those previously described for related complexes based on enediamido ligands,<sup>19</sup> but its coordination mode is surprisingly different. In fact, in previously reported enediamido complexes,<sup>12</sup> the C=C bonds of NCCN moieties are involved in the metal–ligand bonding, while in complex **1** no short  $\text{Y}\cdots\text{C}$  contacts are observed and the metallacycle YNCCN is nearly planar.

Transparent orange crystals of **2** suitable for X-ray diffraction studies were obtained by slow cooling of a DME–hexane solution to  $-20$  °C. The molecular structure of **2** is shown in Figure 2, and the crystal and structure refinement data are summarized in Table 1. Complex **2**, which crystallizes in the monoclinic space group  $P2_1/c$  with four molecules in the unit cell, adopts also a monomeric structure in the solid state. The coordination sphere of the yttrium atom is set up by the two nitrogen atoms of the chelating  $\text{DAB}^{2-}$  ligand and the four oxygen atoms of DME and THF molecules and of the terminal *tert*-butoxide group. In addition, two short  $\text{Y}\cdots\text{C}$  contacts (Y(1)–C(15) 2.703(2), Y(1)–C(13) 2.704(2) Å) are observed. The length of the covalent Y–O bond in **2** (2.067(2) Å) falls in the range of values (1.995(10)–2.124(6) Å) measured for yttrium *tert*-

(15) (a) Ephritikhine, M. *Chem. Rev.* **1997**, *97*, 2193–2242. (b) Schumann, H.; Keitsch, M. R.; Demtschuk, J.; Mühle, S. *Z. Anorg. Allg. Chem.* **1998**, *624*, 1811–1818.

(16) (a) Roesky, P. W. *Organometallics* **2002**, *21*, 4756–4761. (b) Skinner, M. E. G.; Mountford, P. *J. Chem. Soc., Dalton Trans.* **2002**, 1694–1703. (c) Bambirra, S.; Boot, S. J.; van Leusen, D.; Meetsma, A.; Hessen, B. *Organometallics* **2004**, *23*, 1891–1898. (d) Runte, O.; Priemeier, T.; Anwander, R. *Chem. Commun.* **1996**, 1385–1386. (17) Cope-Eatough, E. K.; Mair, F. S.; Pritchard, R. G.; Warren, J. E.; Woods, R. J. *Polyhedron* **2003**, *22*, 1447–1454. (18) Allen, F. A.; Konnard, O.; Watson, D. G.; Brammer, L.; Orpen, G.; Taylor, R. J. *J. Chem. Soc., Perkin Trans.* **1987**, 1–19. (19) (a) Trifonov, A. A.; Borovkov, I. A.; Fedorova, E. A.; Fukin, G. K.; Larionova, J.; Druzhkov, N. O.; Cherkasov, V. K. *Chem.–Eur. J.* **2007**, *13*, 4981–4987. (b) De Waele, P.; Jazdzewski, B. A.; Klosin, J.; Murray, R. E.; Theriault, C. N.; Vosejпка, P. C.; Petersen, J. L. *Organometallics* **2007**, *26*, 3896–3899. (c) Görls, H.; Neumüller, B.; Scholz, A.; Scholz, J. *Angew. Chem., Int. Ed. Engl.* **1995**, *34*, 673–676.

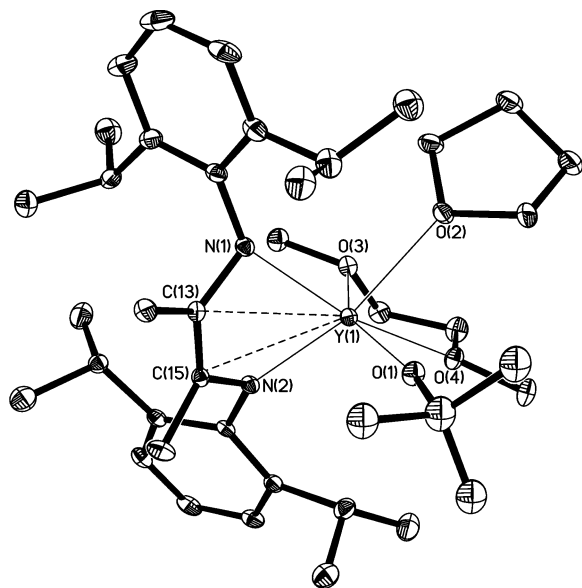


**Figure 2.** Molecular structure of  $\{\text{DAB}\}\text{Y}(\text{OrBu})(\text{THF})(\text{DME})$  (**2**) with 30% ellipsoid probability. Selected distances ( $\text{\AA}$ ) and angles (deg):  $\text{Y}(1)-\text{O}(1)$  2.067(2),  $\text{Y}(1)-\text{O}(2)$  2.439(2),  $\text{Y}(1)-\text{O}(3)$  2.524(1),  $\text{Y}(1)-\text{O}(4)$  2.481(2),  $\text{Y}(1)-\text{N}(1)$  2.229(2),  $\text{Y}(1)-\text{N}(2)$  2.249(2),  $\text{Y}(1)-\text{C}(13)$  2.704(2),  $\text{Y}(1)-\text{C}(15)$  2.703(2),  $\text{N}(1)-\text{C}(13)$  1.423(3),  $\text{N}(2)-\text{C}(15)$  1.427(3),  $\text{C}(13)-\text{C}(15)$  1.376(3),  $\text{N}(1)-\text{Y}(1)-\text{N}(2)$  81.65(6),  $\text{O}(1)-\text{Y}(1)-\text{O}(2)$  91.03(6),  $\text{O}(1)-\text{Y}(1)-\text{O}(4)$  85.62(6).

butoxide complexes with a terminal alkoxide group.<sup>7,20</sup> The  $\text{Y}-\text{N}$  bond distances (2.2290(17) and 2.2485(17)  $\text{\AA}$ ) are similar to those observed in complex **1**. The bonding situation within the planar NCCN fragment ( $\text{N}(1)-\text{C}(13)$  1.423(3),  $\text{N}(2)-\text{C}(15)$  1.427(3),  $\text{C}(13)-\text{C}(15)$  1.376(3)  $\text{\AA}$ ) in **2** is analogous to that in **1** and further confirms the dianionic character of the  $\text{DAB}^{2-}$  ligand. However, the coordination mode of the enediamido fragment in **2** differs essentially from that in **1**; unlike in the latter complex, two short  $\text{Y}\cdots\text{C}$  contacts ( $\text{Y}(1)-\text{C}(15)$  2.703(2),  $\text{Y}(1)-\text{C}(13)$  2.704(2)  $\text{\AA}$ ) are observed in **2**, which reflect  $\eta^2$ -coordination of the  $\text{C}=\text{C}$  bond to the yttrium atom. This interaction transforms drastically the geometry of the YNCCN metallacycle: the yttrium atom goes out of the plane of the NCCN fragment (0.288  $\text{\AA}$ , compared to 0.049  $\text{\AA}$  in **1**); also, the dihedral angle between the  $\text{N}(1)\text{Y}(1)\text{N}(2)$  and  $\text{N}(1)\text{C}(13)\text{C}(15)\text{N}(2)$  planes widens up to 51.3°, instead of 7.8° in **1**. The values for the related dihedral angles in complexes  $\{[\text{HCNC}_6\text{H}_3\text{iPr}_2]\}_2\text{YbCp}^*$  ( $\text{THF}$ ) ( $\text{Cp}^* = \text{C}_5\text{Me}_5$ ,  $\text{C}_5\text{Me}_4\text{H}$ ; 45.2 and 45.6°, respectively),<sup>19</sup> which feature a similar bonding between the metal atom and enediamido ligand, are noticeably smaller than that in complex **2**.

To obtain a better insight into the reason for the different coordination modes of the  $\text{DAB}^{2-}$  ligand in complexes **1** and **2**, an attempt to estimate the steric saturation degree of the yttrium centers employing the ligand solid angle computation approach ( $G$  parameter) was done.<sup>21</sup> The calcula-

tions showed that both complexes are almost sterically saturated with  $G$  parameter values of 93.0(2) and 90.2(2)%, respectively. The overall contributions of the ligands with the exception of the  $\text{DAB}^{2-}$  fragment into the metal atom shielding were found to be 52.3(2)% for **1** and 50.8(2)% for **2**, thus reflecting the lesser extent of steric saturation of the coordination sphere of yttrium in **2**. Taking into account the fact that the contribution of the  $\eta^4$ -coordinated NCCN fragment into the metal atom shielding (29.8(2)%) is noticeably higher compared to that of  $\eta^2$ -coordinated (25.8(8)%), one can conclude that realization of  $\eta^4$ -coordination mode in complex **2** is preferable since it allows reaching a higher degree of steric saturation of the yttrium atom coordination sphere. On the other hand, preliminary estimations of the electronic factor influence based on DFT calculations<sup>22</sup> at the B3LYP/DGDZVP level were done for complexes **1** and **2** (for **2**, the structures with and without  $\text{C}=\text{C}$  bond coordination were compared) and showed that the energy decreases by approximately 7  $\text{kcal}\cdot\text{mol}^{-1}$  as a result of the additional interaction of the yttrium cationic center with the  $\text{C}=\text{C}$  bond (in **2**). Apparently, in complex **1**, despite the energetic advantage, the  $\eta^4$ -coordination mode cannot be realized due to excessive steric hindrance in the yttrium coordination sphere.

Transparent yellow-orange crystals of complex **3** suitable for X-ray diffraction studies were grown by slow condensation of hexane into a DME solution of **3**. This complex crystallizes in the orthorhombic space group  $Pbca$  with eight molecules in the unit cell. The molecular structure of **3** is depicted in Figure 3, and the crystal and structural refinement data are listed in Table 1. In the solid state, compound **3** is an ionic complex made of the discrete cation  $\text{Li}(\text{DME})_3^+$  and complex anion  $\{\{\text{DAB}\}\text{Y}(\text{BH}_4)_2\}^-$ . Both  $\text{BH}_4^-$  groups are  $\mu^3$ -bonded to the yttrium atom via three hydrogen atoms. The  $\text{Y}-\text{B}$  distances (2.552(3) and 2.578(3)  $\text{\AA}$ ) are shorter than the corresponding contacts in yttrium borohydride complexes ( $\text{C}_5\text{Me}_4\text{Et})_2\text{Y}(\text{BH}_4)(\text{THF})$  (2.669(4)  $\text{\AA}$ )<sup>15b</sup> and  $\text{Y}(\text{BH}_4)_3(\text{THF})_3$  (2.58(1) and 2.68(2)  $\text{\AA}$ ).<sup>23</sup> The  $\text{Y}-\text{N}$  bond lengths in **3** (2.167(2) and 2.168(2)  $\text{\AA}$ ) are noticeably shorter than those in **1** and **2**. Analysis of the geometrical features within the NCCN moiety confirmed its dianionic nature. Like in complex **2**, the  $\text{C}=\text{C}$  bond of the  $\text{DAB}^{2-}$  fragment is  $\eta^2$ -coordinated to the yttrium atom and the  $\text{Y}-\text{C}$  distances (2.584(2) and 2.591(2)  $\text{\AA}$ ) are significantly shorter compared to those observed in **2**. The dihedral angle between the  $\text{NYN}$  and the NCCN planes in complex **3** amounts to 56.5°, and the deviation of the  $\text{Y}$  center from the NCCN plane is 0.323  $\text{\AA}$ . The  $G$ -parameter of the anionic part of **3** was found to have a rather low value (74.3(2)%). Such a steric unsaturation of the yttrium coordination sphere can be related to the shortening of the  $\text{Y}-\text{B}$  and  $\text{Y}-\text{N}$  distances.

(20) (a) Evans, W. J.; Boyle, T. J.; Ziller, J. W. *Organometallics* **1993**, *12*, 3998–4009. (b) Evans, W. J.; Sollberger, M. S.; Hanusa, T. P. *J. Am. Chem. Soc.* **1988**, *110*, 1841–1850.

(21) (a) Guzei, I. A.; Wendt, M. *Dalton Trans.* **2006**, *33*, 3991–3999. (b) Fukin, G. K.; Guzei, I. A.; Baranov, E. V. *J. Coord. Chem.* **2007**, *60*, 937–944. (c) Fukin, G. K.; Guzei, I. A.; Baranov, E. V. *J. Coord. Chem.* **2008**, *61*, 1678–1688.

(22) Optimization of the  $[\text{Y}-\text{DAB}]^+$  fragments in **1** and **2** were performed using Gaussian 03 package on the basis of the X-ray geometry of complexes **1** and **2**.

(23) Segal, B. G.; Lippard, S. J. *Inorg. Chem.* **1978**, *17*, 844–850.

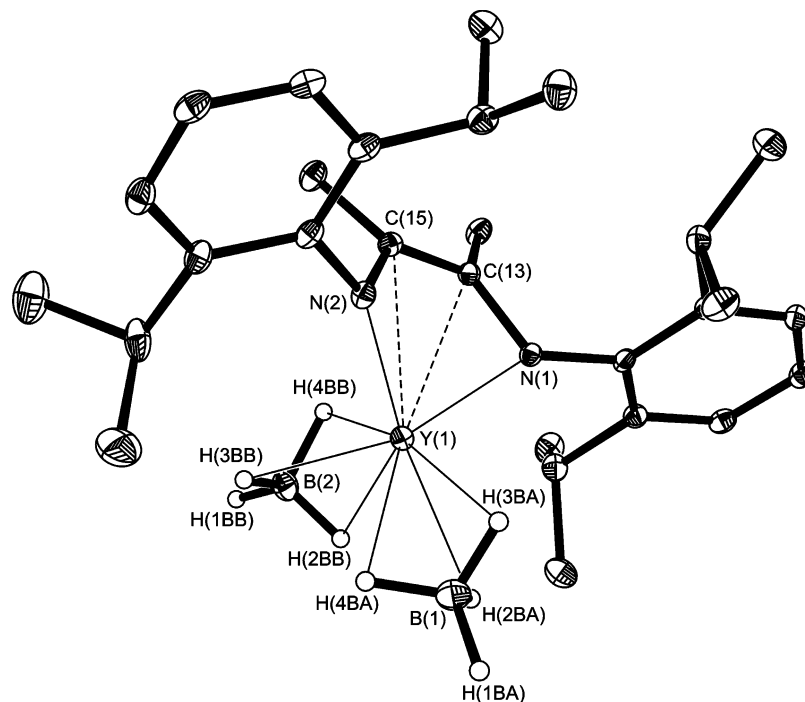
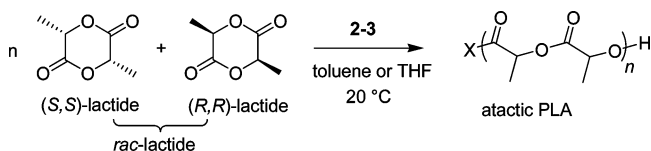


**Figure 3.** Molecular structure of the anionic part  $\{[DAB]Y(BH_4)_2\}^-$  of complex **3** with 30% ellipsoid probability. Selected distances (Å) and angles (deg): Y(1)–N(2) 2.167(2), Y(1)–N(1) 2.168(2), Y(1)–B(1) 2.552(3), Y(1)–B(2) 2.578(3), Y(1)–C(15) 2.584(2), Y(1)–C(13) 2.591(2), Y(1)–H(4BA) 2.42(3), Y(1)–H(2BA) 2.30(4), Y(1)–H(3BA) 2.30(3), Y(1)–H(2BB) 2.38(3), Y(1)–H(3BB) 2.41(3), Y(1)–H(4BB) 2.33(3), N(1)–C(13) 1.413(3), N(2)–C(15) 1.434(3), C(13)–C(15) 1.377(3).

#### Scheme 2



**Preliminary Investigations in the Ring-Opening Polymerization of *rac*-Lactide and *rac*- $\beta$ -Butyrolactone.** The prepared complexes **2** and **3**, which have a potentially initiating group (*O**t*Bu<sup>24</sup> and BH<sub>4</sub>, respectively) have been evaluated in the ROP of *rac*-lactide (LA; Scheme 2). Representative results are summarized in Table 2. Both complexes proved to be active at room temperature, leading to atactic PLAs, as determined by NMR analysis.

In the case of borohydride complex **3**, approximately twice higher reaction rates were observed in an apolar, noncoordinating solvent such as toluene than in THF (turnover frequency = ca. 16 h<sup>-1</sup> in THF vs ca. 35 h<sup>-1</sup> in toluene at 60–70% conv.; entries 1, 2).<sup>25</sup> It is assumed that the latter solvent, because of its high affinity for oxophilic metals such

as group 3 metals and lanthanides, competes with the lactide monomer in the coordination onto the metal center, thus accounting for the longer completion times. Similar detrimental effect of THF in the rate of ROP reactions promoted by group 3 metal complexes has been often observed.<sup>4a–d</sup> However, it is noteworthy that Mountford et al. have observed an opposite trend for the ROP of lactides with lanthanide borohydride complexes supported by diamino-bis(phenolate) ligands;<sup>4i</sup> that is, polymerization rates are higher in THF than in toluene, which is much more seldom observed.<sup>7</sup> Whatever the solvent used, the PLAs produced with **3** showed monomodal distributions, as revealed by SEC analysis. The PLAs had narrow molecular weight distributions ( $M_w/M_n = 1.18–1.24$ ) and average number molecular weights ( $M_n$ ) in close agreement with the theoretical  $M_n$  values, calculated on the assumption that a single HBH<sub>3</sub> group initiates the polymerization; that is, a single PLA chain is produced per yttrium center.<sup>6</sup> This observation reflects the single-site behavior of **3**, comparable to that previously reported for lanthanide borohydride *ate* complexes supported by bulky guanidinate ligands,  $[(Me_3Si)_2NC(N-Cy)_2]_2Ln(\mu-BH_4)_2Li(THF)_2$  (Ln = Nd, Sm, Yb).<sup>6</sup>

The *tert*-butoxide<sup>24</sup> complex **2** showed activity of the same magnitude as that of **3** under similar conditions (entries 3–6). A simple kinetic analysis by NMR monitoring revealed, however, quite different situations according to the nature of the solvent (Figure 4). In fact, the ROP of *rac*-lactide initiated with **2** features an apparent first order in monomer when the reaction is run in THF ( $[rac-LA] = 3.0$  M,  $k_{app} = 0.488$  h<sup>-1</sup> mol<sup>-1</sup> L;  $[rac-LA] = 1.0$  M,  $k_{app} = 0.189$  h<sup>-1</sup> mol<sup>-1</sup> L;  $[rac-LA] = 0.2$  M,  $k_{app} = 0.064$  h<sup>-1</sup> mol<sup>-1</sup> L), while it is apparently zero-order in monomer when the

(24) Our recent investigations on bis(guanidinate) alkoxide complexes of lanthanides (Y, Nd, Lu) have shown that no evident differences in the performances (activity, control over the molecular weights, and molecular weight distributions) of *tert*-butoxide and *iso*-propoxide complexes [for a given metal] could be discerned in the ROP of lactide; see ref 7. Although only the *tert*-butoxide complex was prepared and investigated in ROP in the present study, an overall similar behavior can be anticipated for the *iso*-propoxide analogue  $\{DAB\}Y(OiPr)(THF)(DME)$ .

(25) A blank experiment using LiBH<sub>4</sub> showed that this compound is not active for the ROP of *rac*-lactide under the conditions used. This observation is in line with previous observations in the ROP of cyclic esters ( $\epsilon$ -caprolactone) and carbonates (TMC) [S. Guillaume, personal communication] and discards the possibility that ROP is initiated by LiBH<sub>4</sub> arising from dissociation of complex **1**.

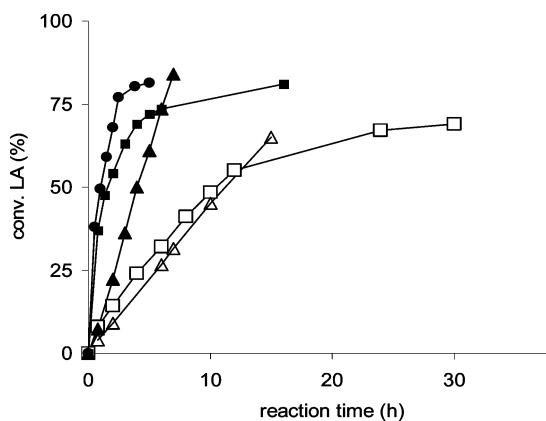


**Figure 4.** Plot of the *rac*-LA conversion with complex **2** as a function of reaction time with  $[rac\text{-LA}]/[\mathbf{2}] = 500$  at 20 °C; in toluene solution (▲,  $[rac\text{-LA}] = 1.0$  M; △,  $[rac\text{-LA}] = 0.2$  M); and in THF solution (●,  $[rac\text{-LA}] = 3.0$  M; ■,  $[rac\text{-LA}] = 1.0$  M; □,  $[rac\text{-LA}] = 0.2$  M).

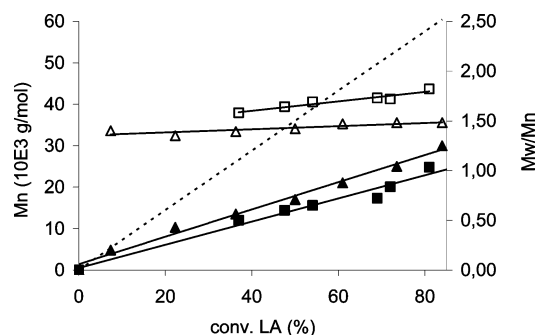


**Figure 5.** Plots of experimental (SEC-RI) average molecular weights (▲, toluene solution; ■, THF solution) and molecular weight distributions (△, toluene solution; □, THF solution) of PLAs produced with complex **2** as a function of *rac*-LA conversion ( $[rac\text{-LA}]/[\mathbf{2}] = 500$ ,  $[rac\text{-LA}] = 1.0$  M, 20 °C); the dashed line represents calculated  $M_n$  values for a perfectly living polymerization.

reaction is run in toluene ( $[rac\text{-LA}] = 1.0$  M,  $k_{app} = 0.123$  h<sup>-1</sup>;  $[rac\text{-LA}] = 0.2$  M,  $k_{app} = 0.0087$  h<sup>-1</sup>).<sup>26</sup> In other words, there is a change in the rate-determining step (rds); in THF, the rds involves lactide and is likely to be the coordination of lactide onto the yttrium center, in competition with THF as above-mentioned. In toluene, the rds does not involve the concentration of monomer in solution and may be either ring-opening of the coordinated monomer by nucleophilic migration of the alkoxide group onto the monomer carbonyl function, ring-opening of a tetrahedral intermediate, or dissociation of coordinated polymer chain ketone from the metal center to open a coordination site.

The PLAs produced with **2** in toluene or in THF had relatively broad molecular weight distributions ( $M_w/M_n = 1.5\text{--}2.0$ ), which remained constant over the polymerization course (Table 2, Figures 5 and 6). The molecular weights increased monotonously with the lactide conversion but were systematically lower than those calculated on the assumption that a single PLA chain is produced per metal center via initiation of the polymerization by the *tert*-butoxide group (Table 2, Figure 5). This observation is indicative of a

significant degree of chain transfer (back-biting), as confirmed by MALDI-TOF-MS.<sup>27</sup>

The nature of the actual initiating group was assessed by NMR spectroscopy in the case of *tert*-butoxide complex **2**;<sup>28</sup> use of *tert*-butoxide initiators in ROP of cyclic esters<sup>7</sup> remains much less documented than with other alkoxides such as isopropoxides and benzyloxides.<sup>24</sup> The <sup>1</sup>H NMR spectrum in CDCl<sub>3</sub> of a relatively low molecular weight sample of PLA (Table 2, entry 3) shows the [broadened] quartet characteristic of the CH(Me)OH terminal group at δ 4.38 ppm (as well as a broad signal at δ 2.69 ppm for CH(Me)OH; see the Supporting Information). The latter group is formed after hydrolysis of the metal–alkoxide bond, an observation which is indicative of a classical coordination/insertion mechanism with an initial ring-opening via acyl-oxygen bond cleavage.<sup>29</sup> The observation of a singlet resonance at δ 1.47 ppm, expectedly more intense, establishes the presence of a *tert*-butoxycarbonyl function at the other terminus of the PLA chain. This assignment was supported by <sup>13</sup>C NMR spectroscopy (δ 69.4 ppm, OC(CH<sub>3</sub>)<sub>3</sub> and δ 27.9 ppm, OC(CH<sub>3</sub>)<sub>3</sub>; see the Supporting Information).

The possibility to achieve immortal polymerization with these systems, that is, to generate several PLA chains per metal center by introducing several equivalents of a chain transfer agent, was explored with complex **2** in the presence of *iso*-propanol (Table 2, entries 7–11) (Scheme 3).<sup>4d</sup> This system proved able to convert quantitatively 500 equiv of lactide with up to 50 equiv of chain transfer agent per metal initiator. All the obtained PLAs showed monomodal, relatively narrow distributions with  $M_n$  values decreasing with increasing amounts of isopropanol, though there was no strict proportionality between these values. To prove the good productivity of these catalyst systems, experiments were performed using up to 2000 equiv of *rac*-LA per yttrium, in the presence of 5 equiv of *iso*-propanol (Table 2, entries 10 and 11). High conversions and, in turn, high molecular weight polymers could be obtained with a good degree of control. Thus, DAB<sup>2-</sup> appears to be a good ligand for stabilizing the oxophilic yttrium center, preventing irreversible decomposition in the presence of a large excess of free alcohol. The overall efficiency of chain transfer with Y-DAB complexes is almost as good as what we recently reported using lanthanide–alkoxide complexes supported by guanidinate ligands.<sup>7</sup> One must bear in mind that metal systems which allow achieving immortal ROP of lactide, that is, to

(26) From these data, the order in catalyst (**2**) and rate constant were roughly estimated as  $n = 0.74 \pm 0.09$  and  $k = 20.95 \pm 5$  h<sup>-1</sup> in THF, and  $n = 1.65 \pm 0.2$  and  $k = 3390 \pm 650$  h<sup>-1</sup> in toluene, respectively.

(27) MALDI-TOF-MS analysis of some PLA samples showed distributions containing both even-membered and odd-membered oligomers, with peaks separated by 72 Da; this unambiguously establishes that transesterification processes actually take place in these systems.

(28) The nature of the terminus groups in PLAs produced with borohydride complex **3** could not be unambiguously identified. <sup>1</sup>H and <sup>13</sup>C NMR spectroscopy suggested that mixtures of PLAs having mostly CH<sub>2</sub>OH and possibly also CHO termini are the main products. For end-group analysis of polyesters produced from borohydride initiators, see: (a) Palard, I. A. S.; Guillaume, S. M. *Chem.-Eur. J.* **2004**, 4054–4062. (b) Guillaume, S. M.; Schappacher, M.; Soum, A. *Macromolecules* **2003**, 36, 54–60. (c) Palard, I.; Soum, A.; Guillaume, S. M. *Macromolecules* **2005**, 38, 6888–6894. (d) See ref 4i.

(29) (a) Kricheldorf, H. R.; Berl, M.; Scharnagi, N. *Macromolecules* **1988**, 21, 286–293. (b) Dubois, P.; Jacobs, C.; Jérôme, R.; Teyssié, P. *Macromolecules* **1991**, 24, 2266–2270.



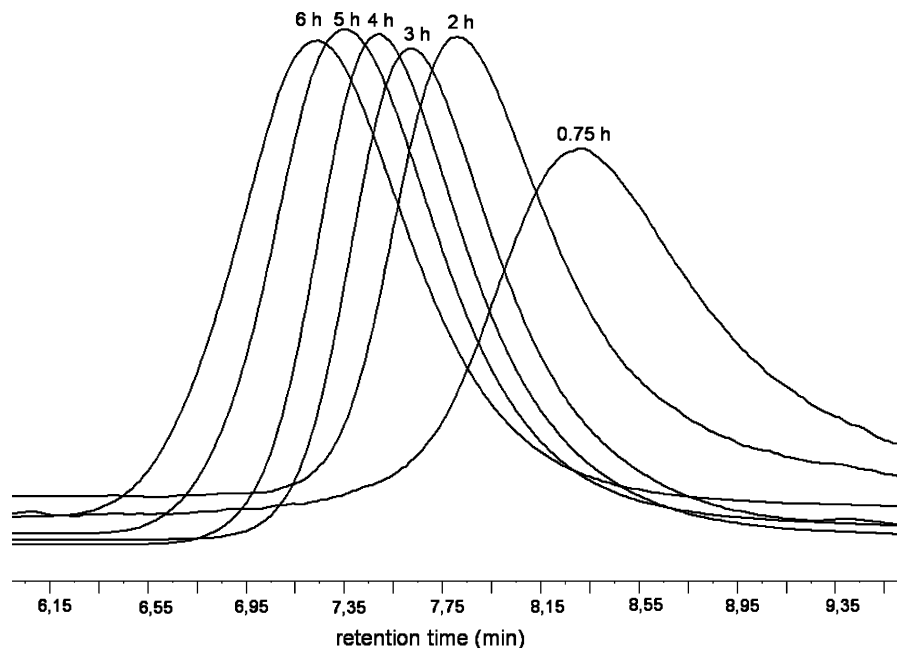
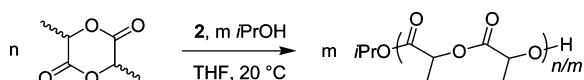
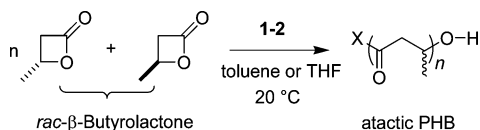


**Figure 6.** SEC-RI traces (THF, 25 °C) of PLAs produced by **2** as a function of time ( $[rac\text{-LA}]/[\mathbf{2}] = 500$ ,  $[rac\text{-LA}] = 1.0$  M in toluene, 20 °C).

#### Scheme 3



#### Scheme 4



make true catalysis and to grow as many as 50 polymer chains per metal center, remain quite uncommon so far.

The ROP of *rac*- $\beta$ -butyrolactone was also briefly investigated (Scheme 4). Representative results are summarized in Table 3. Interestingly, both complexes **2** and **3** showed activity under mild conditions (20 °C). The reactions proceeded slowly, limiting the molecular weights of the final poly(3-hydroxybutyrate)s (PHBs). The  $M_n$  values of the PHBs determined by SEC were in overall good agreement with the calculated values based on the growth of a polymer chain per metal center, and the molecular distributions were quite narrow. Those observations further corroborate the single-site character of the [Y-DAB] systems. Detailed analysis of the carbonyl region of the  $^{13}\text{C}$  NMR spectra also showed that those PHBs have an atactic microstructure (see the Supporting Information).

#### Conclusions

In conclusion, we have described the synthesis and structural features of new yttrium chloride, alkoxide, and borohydride complexes supported by a linked diamido ligand.

The coordination modes of the enediamido fragment onto the yttrium centers in complexes **1–3** differ considerably by the bonding situation and extent of steric saturation of the metal coordination sphere. In complex **1**, the  $\text{DAB}^{2-}$  ligand is bonded to the metal center via two covalent Y–N bonds, while in complexes **2** and **3** additional  $\eta^2$ -coordination of the C=C bond to the metal atom is observed, both in solution and in the solid state. The borohydride and *tert*-butoxide complexes **2** and **3** act as monoinitiators for the room temperature ring-opening polymerization of racemic lactide and  $\beta$ -butyrolactone, providing atactic polymers with a certain degree of control, that is, controlled molecular weights and relatively narrow polydispersities. The  $\text{DAB}^{2-}$  ligand appears to be a remarkably stabilizing ligand of yttrium, enabling it to perform immortal ROP of lactide with as many as 50 equiv of isopropanol per metal center, thus enhancing by the same factor the catalytic efficiency of the Y-DAB complex.

**Acknowledgment.** This work was supported by the GDRI “CH2D” between RAS and CNRS, by the Russian Foundation for Basic Research (Grant No 08-03-00391-a, 06-03-32728), Program of the Presidium of the Russian Academy of Science (RAS), RAS Chemistry and Material Science Division, and the *Institut Universitaire de France* (IUF).

**Supporting Information Available:** The molecular structure of complexes **1**, **2**, and **3** as CIF files; additional  $^1\text{H}$  and  $^{13}\text{C}$  NMR spectra of PLAs and PHBs. This material is available free of charge via the Internet at <http://pubs.acs.org>.

IC802427F